

Neutron correlations in ${}^6\text{He}$ viewed through nuclear break-up

M. Assié^{1,a}, J.A. Scarpaci¹, D. Lacroix², J.C. Angélique³, D. Bazin⁴, D. Beaumel¹, Y. Blumenfeld¹, W.N. Catford⁵, M. Chabot¹, A. Chatterjee⁹, M. Fallot⁶, H. Iwasaki¹, F. Maréchal¹, D. Mengoni⁷, C. Monrozeau¹, J. Nyberg⁸, C. Petrache¹, F. Skaza¹, and T. Tuna¹

¹ Institut de Physique Nucléaire, Université Paris-Sud-11-CNRS/IN2P3, 91406 Orsay, France

² GANIL, BP 5027, 14076 Caen Cedex 5, France

³ LPC/ENSICAEN, Blvd du Maréchal Juin, 14050 Caen Cedex, France

⁴ National Superconducting Cyclotron Laboratory, Michigan State University, East-Lansing, MI 48824-1321, USA

⁵ School of Electronics and Physical Sciences, University of Surrey, Guildford GU2 7XH, UK

⁶ Subatech, 4 rue Alfred Kastler BP 20722, F-44307 Nantes Cedex 3, France

⁷ Dipartimento di Fisica, Università di Camerino and INFN, Sezione di Perugia, I-62032, Camerino, Italy

⁸ Department of Physics and Astronomy, Uppsala University, Uppsala, Sweden

⁹ Nuclear Physics Division, Bhabha Atomic Research Centre, Mumbai 400085, India

Received: 3 December 2008 / Revised: 19 February 2009

Published online: 10 May 2009 – © Società Italiana di Fisica / Springer-Verlag 2009

Communicated by C. Signorini

Abstract. The nuclear break-up of ${}^6\text{He}$ on a ${}^{208}\text{Pb}$ target was studied at 20 A MeV using a secondary beam of ${}^6\text{He}$ produced by the SPIRAL facility at GANIL. α -particles were detected in coincidence with two neutrons with a large angular coverage and the reaction mechanism was identified. From the distribution of the relative angles between the two neutrons the correlation function was extracted. It shows a strong correlation at small relative angles attributed to the contribution of the di-neutron configuration of ${}^6\text{He}$.

PACS. 24.50.+g Direct reactions – 25.10.+s Nuclear reaction involving few-nucleons systems – 24.10.-i Nuclear reaction models and methods – 25.60.Gc Break up and momentum distributions

1 Introduction

The ${}^6\text{He}$ nucleus is an archetype of three-body nuclear system in which an α core is surrounded by two correlated neutrons. In its ground state, the coexistence of two configurations is predicted: one in which the two neutrons are close together (di-neutron configuration) and one where the two neutrons are on opposite sides with respect to the core (cigar configuration) [1]. A better knowledge of this nucleus should help to understand other drip-line nuclei.

The correlation between the two halo neutrons of ${}^6\text{He}$ have been studied by different experimental techniques. The delayed emission of deuteron observed in the β -decay of ${}^6\text{He}$ [2, 3] is in favor of a di-neutron configuration [4]. On the other hand, with radiative capture of a 40 MeV proton on ${}^6\text{He}$, no decay in the $\alpha + t$ channel was observed indicating rather a cigar configuration [5]. As far as the reaction mechanism is concerned, two-neutron transfer seems to be a powerful tool to study neutron correlation and to extract spectroscopic factors for each configuration. For different targets and beam energies [6–11] the 2n transfer cross-section could be understood within DWBA or

CRC calculations including only direct 2n transfer and therefore suggesting a di-neutron configuration. The contribution of the two-step transfer [12] and of the triton transfer [9], respectively, seem to be very low. Coulomb break-up reactions have also been performed at 40 A MeV and the distance between the two neutrons was extracted using the method of neutron interferometry [13]. A relative distance between the two neutrons of 5.9 ± 1.2 fm was found suggesting a cigar configuration for the two neutrons. From the above discussion, it is clear that there is no consensus between all the results on the ${}^6\text{He}$ configuration obtained through different reaction mechanisms.

2 Nuclear break-up as a probe for correlations

Nucleon emission from ${}^6\text{He}$ induced by nuclear perturbation of a target during a collision is expected to vary significantly with initial correlations of the two neutrons in ${}^6\text{He}$, making nuclear break-up an interesting reaction mechanism to study correlations.

One-neutron nuclear break-up has already been proposed as a tool for spectroscopic studies [14]. A time-dependent non-perturbative calculation solving the

^a e-mail: assie@ganil.fr

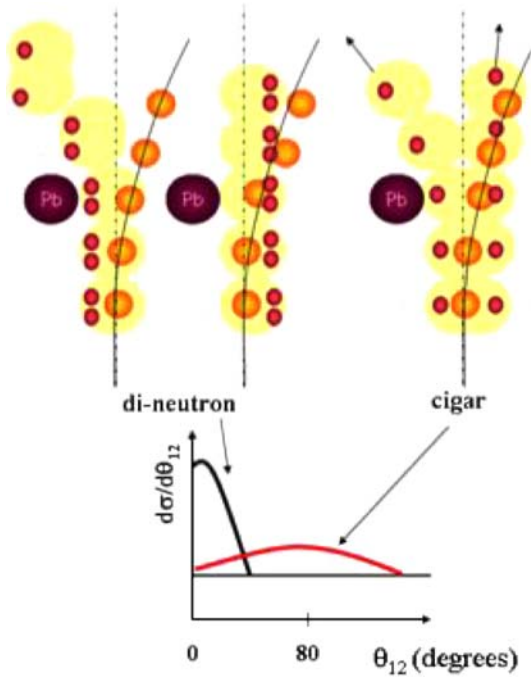


Fig. 1. Intuitive picture of the nuclear break-up of ${}^6\text{He}$ in the di-neutron and the cigar configuration. When the two nucleons are close to each other, their relative angle after emission is small whereas it is large when they are on opposite sides with respect to the core.

Schrödinger equation (TDSE) [15] showed that nuclear break-up leads to emission of a nucleon at large angle with a typical emission pattern where the remnant core and the towed nucleon are expected on opposite sides with respect to the beam axis. This phenomenon was already observed for stable nuclei [14] and for the one-neutron halo nucleus ${}^{11}\text{Be}$ [16] where it showed a strong cross-section of about 0.5 barns. Moreover, this mechanism appears to be very sensitive to the quantum properties of the emitted neutron.

As far as neutron correlations are concerned, nuclear break-up should disentangle the two configurations of ${}^6\text{He}$ as depicted in fig. 1. In the di-neutron configuration, both neutrons will be attracted by the target and a much closer emission in phase-space is expected leading to small relative angle between the two neutrons. In the cigar configuration, only one of the two neutrons is expected to feel significantly the nuclear target potential while the other will follow the quasi-projectile and will be emitted along its direction as depicted at the right side of fig 1. From this simple picture of nuclear break-up, the distribution of relative angles between the two neutrons is expected to depend strongly on initial neutrons configuration (see bottom of fig. 1).

The nuclear break-up of correlated nucleons has been theoretically studied for ${}^{16}\text{O}$ using a time-dependent transport model based on the mean-field approach and taking into account 2p-2h correlations [17]. This model is based on the Time-Dependent Density Matrix (TDDM) theory [18,19] with the assumption that correlations are dominant for pairs of time-reversed single-particle wave

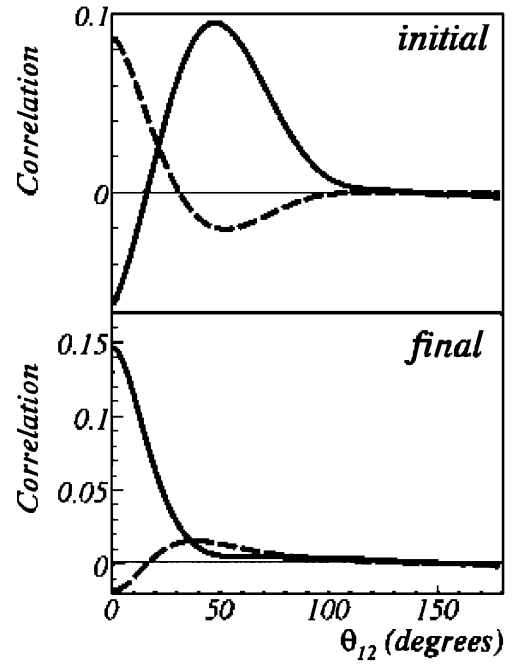


Fig. 2. Two-body correlation as a function of the relative angle between the two neutrons at initial and final time of the dynamical evolution for ${}^{16}\text{O}$ using an attractive (full line) or a repulsive (dashed line) residual interaction.

functions. Within this approach, only the last two neutrons of ${}^{16}\text{O}$ were considered to create two-body correlations. To mimic nucleons which are close (respectively, well-separated) in phase-space, we have used an attractive ($v_0 = -300 \text{ MeV fm}^3$) (respectively, repulsive ($v_0 = +300 \text{ MeV fm}^3$)) schematic interaction of the form

$$v_{12}(\mathbf{r}_1, \mathbf{r}_2) = v_0 \left(1 - \frac{1}{2} \frac{\rho}{\rho_0} \right) \delta(\mathbf{r}_1 - \mathbf{r}_2),$$

where $\rho_0 = 0.16 \text{ fm}^{-3}$ is the normal density. The attractive force gives a di-neutron-type configuration and the repulsive force a cigar configuration. At the initial time the attractive force leads to close neutrons in coordinate space and a large relative angle in momentum space whereas the repulsive force leads to large distance between the two neutrons and small relative angle in momentum space (see top of fig. 2). In this calculation, the two-body correlations at initial and final time of the dynamical evolution have been extracted in momentum space. In fig. 2, the correlated part of the emission is shown as a function of relative angle between the two neutrons, θ_{12} , defined by

$$\cos \theta_{12} = \cos \theta_1 \cos \theta_2 + \sin \theta_1 \sin \theta_2 \cos(\phi_1 - \phi_2),$$

where (θ_i, ϕ_i) are the coordinates of the i -th neutron.

For both configuration, the correlation looks very different after the break-up has occurred than before it, showing the effect of the dynamics in this process. Moreover, the attractive force (di-neutron configuration) leads to an emission at a small relative angle and the repulsive force

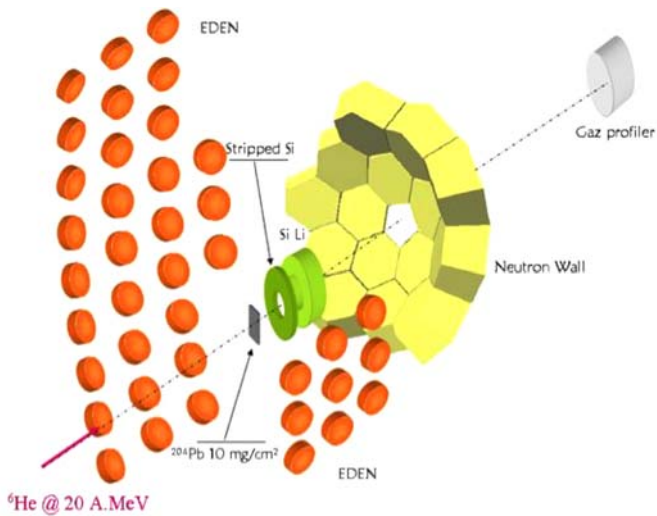


Fig. 3. Experimental set-up.

(cigar configuration) leads to an emission at a larger relative angles confirming the scenario given in fig. 1. This theoretical calculation shows that nuclear break-up is sensitive to the initial correlations of the neutrons so that it will be able to probe neutron correlations in ${}^6\text{He}$.

3 Experimental set-up

The nuclear break-up of ${}^6\text{He}$ on a ${}^{208}\text{Pb}$ target was performed at the GANIL facility. The ${}^6\text{He}$ beam was produced by the ISOL technique and accelerated at 20 A MeV by the CIME cyclotron at the SPIRAL facility [20] with an average intensity of 5×10^6 pps. The target was a 10 mg/cm^2 thick ${}^{208}\text{Pb}$ foil. The experimental set-up is shown in fig. 3. The charged particles were identified using an annular telescope consisting of a double-sided Si-strip ΔE detector with a thickness of $500 \mu\text{m}$ backed with a 3.4 mm thick Si(Li) E detector. The Si-strip detector had 4 quadrants, each with 16 strips made of 2 mm wide rings on the front side and 24 strips made of 3.4 degrees sectors on the rear side. The telescope was located at a distance of 11.8 cm from the target and covered an angular range in the laboratory from 8 to 18 degrees relative to the incoming beam axis. The angular resolution of the telescope was about 1° . The choice of a ${}^{208}\text{Pb}$ target was guided by this detector because the charged particles needed to be deviated enough to be detected.

The ΔE - E plot shown in fig. 4 enables the identification of the ${}^6\text{He}$ beam as well as α -particles originating from break-up.

Regarding the detection of neutrons, a large angular coverage was needed, which was achieved by using two liquid-scintillator-based neutron detector arrays: the Neutron Wall detector [21] and EDEN [22]. The 45 detectors of the Neutron Wall, each with a thickness of about 15 cm , were positioned at 51 cm from the target and were covering $\approx 20\%$ of 4π for angles ranging from 10° to 60° . Due to the thickness of the detectors and the close distance

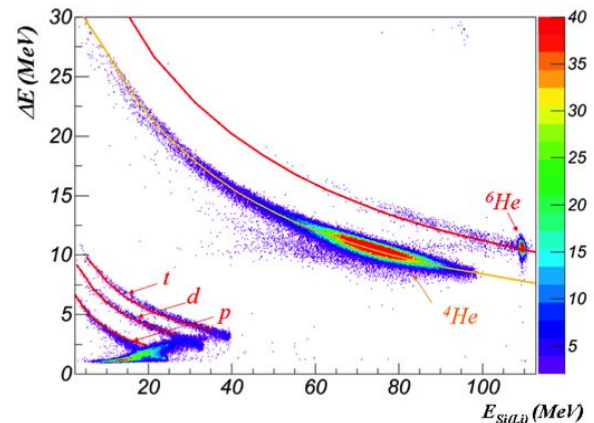


Fig. 4. Correlation between energy loss in the Si-strip detector versus energy loss in the Si-Li detector. ${}^6\text{He}$, α , t , d , p can be identified.

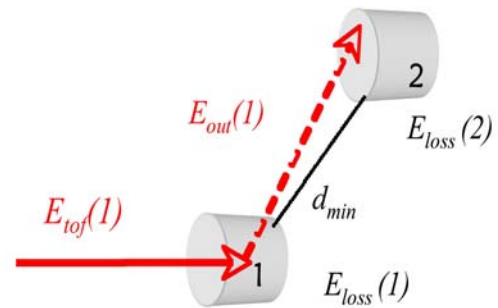


Fig. 5. Crosstalk rejection (see text for details).

to the target, the energy resolution of this detector was about 50% at 20 MeV . At this energy the intrinsic neutron detection efficiency was about 30% .

EDEN detectors, 39 modules of 5 cm thickness and 20 cm in diameter were located on each side of the target at distances ranging from 1.5 m to 1.9 m and covered 3% of 4π from 70° to 110° . The intrinsic efficiency of the EDEN detectors at 20 MeV was about 15% and the energy resolution was about 4% .

Energies of the neutrons were deduced from time-of-flight measurement where the Si-strip detector gave the START signal and the neutron detector the STOP signal. The overall time resolution was about 2.5 ns . The neutron- γ separation was done using the charge comparison and zero-crossover methods for the EDEN and Neutron Wall detectors, respectively.

One of the major issue of the detection of pairs of neutrons is to differentiate a real event from the crosstalk phenomenon [23]. For that purpose, a GEANT4 simulation was performed assuming the detection of one neutron between 5 and 20 MeV . 20% of the events gave crosstalk events in the Neutron Wall while only 5% in EDEN. The crosstalk was reduced according to the algorithm given in [24] with the following rejection conditions being (see fig. 5 for notations):

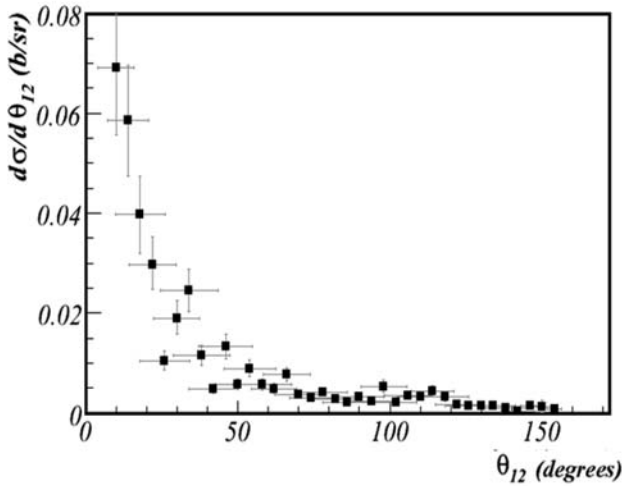


Fig. 6. Differential cross-section as a function of the relative angle between the two neutrons for triple-coincidence events ($\alpha + n + n$) with neutrons of energies larger than 5 MeV.

- the energy deposition in one detector, $E_{loss}(1)$, is greater than the energy obtained from the time of flight, $E_{tof}(1)$: $E_{loss}(1) > E_{tof}(1)$;
- the neutron in the first detector has enough time to go to the second detector and enough energy to make the energy deposit: $E_{out}(1) > E_{loss}(2)$ and $E_{out}(1) > E_{min}$, where $E_{min} = \frac{1}{2}m_n \frac{d_{min}^2}{(t_2 - t_1)^2}$ and t_1 and t_2 correspond to the time of flight of the first and the second neutron, respectively.

For neutrons measured in two neighboring detectors of the Neutron Wall, the second part of the second condition is automatically fulfilled ($E_{min} = 0$). With this algorithm, the GEANT4 simulation shows that only 4% of crosstalk events remain. The distribution of relative angle between the two neutrons, θ_{12} , after this crosstalk rejection procedure is shown in fig. 6 for triple-coincidence events ($\alpha + n + n$). To avoid the contribution of target evaporation, only neutrons of kinetic energies greater than 5 MeV were considered. The peak at angles lower than 30 degrees correspond to 30% of the initial events (no crosstalk events) which is significant compared to the 4% estimated remaining crosstalk events. In order to obtain information on the correlation, this distribution has to be compared to the one that would have been obtained if there was no initial correlation between the neutrons.

4 Angular correlations between emitted neutrons

4.1 Method and tests

The angular correlation function is defined by

$$C_{12}(\theta_{12}) = \frac{P(\theta_{12})}{P(\theta_1)P(\theta_2)}, \quad (1)$$

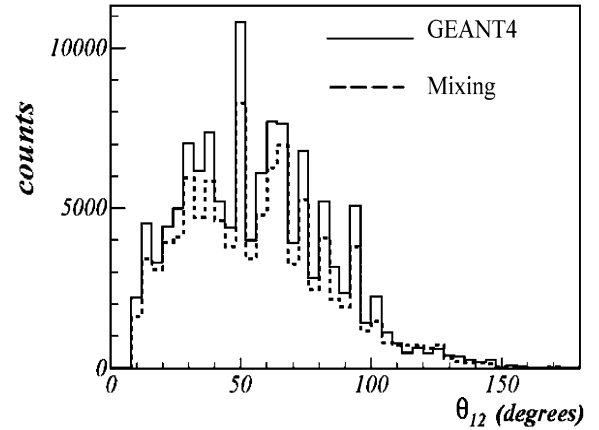


Fig. 7. Distribution obtained by mixing the real events compared with the distribution obtained from a GEANT4 simulation of an isotropic distribution of neutrons with an energy lower than 5 MeV.

where $P(\theta_{12})$ is the experimental distribution and $P(\theta_1)$ $P(\theta_2)$ is the independent emission of one neutron at the angle θ_1 and of another neutron at θ_2 , respectively. The correlation function is equal to 1 if there are no correlations. To get the independent emission probability from the experimental data, an event mixing technique is used. To simulate events with uncorrelated neutrons one neutron is picked up in one experimental event and another from a second event and their relative angle is computed. The two distributions obtained by this method contain the same experimental effects such as the acceptance of the experimental set-up. This method has already been used in refs. [13, 25]. For strongly correlated systems, the event mixing procedure needs several iterations because it may happen that the pairs of neutrons picked up during the mixing are very close to the original experimental event. To avoid this, starting from the second iteration each neutron is weighted by the inverse of its average correlation with all other neutrons in other events [13]. In our case, up to five iterations were necessary for the method to converge.

Tests of the correlation function were performed for neutrons with an energy lower than 5 MeV mainly arising from the target evaporation. The correlation function extracted is compatible with 1 except at very small angles where there is a small correlation. This correlation certainly comes from the remaining neutrons emitted by break-up with energies lower than 5 MeV.

A GEANT4 simulation of our experimental set-up has been performed. An isotropic relative angle distribution of neutrons with an energy lower than 5 MeV was extracted and the distribution obtained is very close to the one obtained with the event mixing technique. The structures in the distribution are not due to statistical fluctuations but they are due to the discretization of relative angles in our experimental set-up (see fig. 7). To avoid these structures, a randomization of the relative angle, based on GEANT4, has been used.

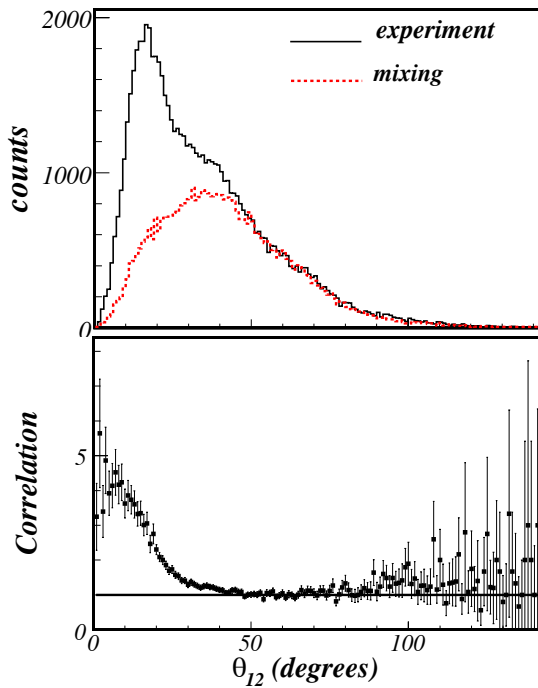


Fig. 8. Top: distribution of relative angle compared to the distribution obtained by mixing events. Bottom: correlation function for neutrons with an energy greater than 5 MeV.

4.2 Correlation function for the total distribution

The correlation function has been extracted from the experimental data for neutrons with an energy greater than 5 MeV (see fig. 8). The experimental and the mixed distributions have different shapes at small relative angles and at large relative angles. In order to extract the correlation, the mixed distribution is normalized to the large relative angles, where no correlation is expected. The correlation shows a strong deviation from 1 at small relative angles. Using instead another normalization (for example, normalizing to the total number of counts), the correlation shape remains the same but the value of each contribution differs.

4.3 Correlation function for nuclear break-up

To select only the contribution due to nuclear break-up in our data, a condition that at least one neutron is emitted at angles larger than 30 degrees is imposed to construct the distribution of the relative angles. The contribution due to the Coulomb break-up is then excluded as its cross-section falls down above 20 degrees in the single-neutron angular distribution and the nuclear break-up dominates.

The correlation function in this case (see fig. 9) shows strong correlation at small relative angle. This contribution is significant and remains dominant for every condition on the emission angle of the neutron. From the calculation shown in fig. 2, we do expect that the di-neutron configuration leads to emission at relative an-

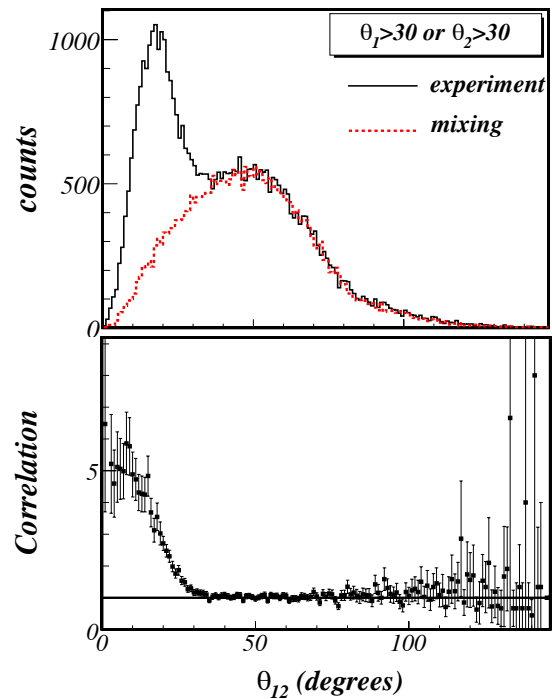


Fig. 9. Distribution of relative angles (top) and correlation function (bottom) for events in which at least one neutron was detected at an angle larger than 30 degrees.

gles lower than 30 degrees, whereas the cigar configuration leads to emission of neutron at relative angles around 30 degrees. Although specific calculation dedicated to the ${}^6\text{He}$ case are needed, a comparison between figs. 8-9 and the schematic/preliminary calculation presented in fig. 2 seems to indicate that no cigar contribution is observed in our experimental data and the small-angle contribution stems from the di-neutron configuration only.

5 Conclusion

Two-neutron correlations in ${}^6\text{He}$ have been studied. The naive picture (fig. 1) of the possibility to observe the di-neutron and cigar configurations of ${}^6\text{He}$ in a nuclear break-up reaction, was predicted by the time-dependent density matrix theory (fig. 2). A clear experimental signature of an enhanced di-neutron component was observed in this work (fig. 9). To further proceed with the study of the configuration mixing in ${}^6\text{He}$ and to extract an upper limit on the cigar configuration, a comparison with a theoretical calculation is necessary. Four-body CDCC calculations of the break-up of ${}^6\text{He}$ on a ${}^{208}\text{Pb}$ target are in progress [26]. In parallel, a time-dependent theory going beyond the mean-field has been developed and applied to oxygen isotopes and an extension to the study of ${}^6\text{He}$ is in progress.

This work was partially supported by the Swedish Research Council. The European Gamma-Ray Spectroscopy Pool is acknowledged for lending us the Neutron Wall equipment.

References

1. M.V. Zhukov *et al.*, Phys. Rep. **231**, 151 (1993).
2. K. Riisager *et al.*, Phys. Lett. B **235**, 30 (1990).
3. M.G. Borge *et al.*, Nucl. Phys. A **560**, 664 (1993).
4. M.V. Zhukov, B.V. Danilin, L.V. Grigorenko, N.B. Shul'gina, Phys. Rev. C **47**, 2937 (1993).
5. E. Sauvan *et al.*, Phys. Rev. Lett. **87**, 042501 (2001).
6. Y. Oganessian, V.I. Zagrebav, J.S. Vaagen, Phys. Rev. Lett. **82**, 044605 (1999).
7. R. Raabe *et al.*, Phys. Lett. B **458**, 1 (1999).
8. R. Wolski *et al.*, Phys. Lett. B **467**, 8 (1999).
9. L. Giot *et al.*, Phys. Rev. C **71**, 064311 (2005).
10. A. Chatterjee *et al.*, Phys. Rev. Lett. **101**, 032701 (2008).
11. R. Raabe *et al.*, Phys. Rev. C **67**, 044602 (2003).
12. D.T. Khoa, W. von Oertzen, Phys. Lett. B **595**, 193 (2004).
13. F.M. Marquès *et al.*, Phys. Lett. B **476**, 219 (2000).
14. J.-A. Scarpaci *et al.*, Phys. Lett. B **428**, 241 (1998).
15. D. Lacroix, J.A. Scarpaci, Ph. Chomaz, Nucl. Phys. A **658**, 273 (1998).
16. V. Lima *et al.*, Nucl. Phys. A **795**, 1 (2007).
17. M. Assié, D. Lacroix, to be published in Phys. Rev. Lett., arXiv: 0901.0848 [nucl-th].
18. S. Wang, W. Cassing, Ann. Phys. **159**, 328 (1985).
19. M. Tohyama, A.S. Umar, Phys. Lett. B **549**, 72 (2002).
20. Spiral group, A.C. Villari, Nucl. Phys. A **693**, 465 (2001).
21. O. Skeppstedt *et al.*, Nucl. Instrum. Methods A **421**, 531 (1999).
22. H. Laurent *et al.*, Nucl. Instrum. Methods A **326**, 517 (1993).
23. J. Ljungvall, M. Palacz, J. Nyberg., Nucl. Instrum. Methods A **528**, 741 (2004).
24. F.M. Marquès, M. Labiche, N.A. Orr, F. Sarazin, J.C. Angélique, Nucl. Instrum. Methods A **450**, 109 (2000).
25. F.M. Marquès *et al.*, Phys. Rev. C **64**, 061301(R) (2001).
26. M. Rodriguez-Gallardo *et al.*, Phys. Rev. C **77**, 064609 (2008).